Techno-economics of Fiber vs. Microwave for Mobile Transport Network Deployments [Invited]

Citation for the original published paper (version of record):
Lashgari, M., Tonini, F., Capacchione, M. et al (2023). Techno-economics of Fiber vs. Microwave for Mobile Transport Network Deployments [Invited]. Journal of Optical Communications and Networking, 15(7): C74-C87. http://dx.doi.org/10.1364/JOCN.482865

(article starts on next page)

Techno-economics of Fiber vs. Microwave for Mobile Transport Network Deployments [Invited]

MARYAM LASHGARI[1,*], FEDERICO TONINI[1], MASSIMILIANO CAPACCHIONE[2], LENA WOSINSKA[1], GABRIELE RIGAMONTI[2], AND PAOLO MONTI[1]

[1] *Department of Electrical Engineering, Chalmers University of Technology, Gothenburg, Sweden*
[2] *SIAE Microelettronica, Cologno Monzese, Italy*
[*] *Corresponding author: maryaml@chalmers.se*

Compiled March 25, 2023

One of the challenges for network operators is to design and deploy cost-efficient transport networks (TNs) to meet the high capacity and strict latency/reliability requirements of today's emerging services. Therefore, they need to consider different aspects, including the appropriate technology, the level of reconfigurability, and the functional split option. A crucial aspect of network design is assessing the impact of these aspects against the total cost of ownership (TCO), latency, and reliability performance of a given solution. For this reason, this paper proposes a framework to investigate the TCO, latency, and reliability performance of a set of fiber and microwave-based TN architectures. They are categorized based on their baseband functional split option and the reconfigurability capabilities of the equipment used. The results, based on real data from a non-incumbent operator, show that in most of the considered scenarios, a microwave-based TN exhibits lower TCO than a fiber-based one. The TCO gain may vary with the choice of the functional split option, geo-type, reconfigurability features, fiber trenching costs, and cost of microwave equipment, with a more significant impact in a dense urban geo-type, where for a low layer functional split option the fiber- and microwave-based architectures have a comparable TCO. Finally, it was found that the considered fiber and microwave architectures have almost similar average latency and connection availability performance. Both are suitable to meet the service requirements of 5G and beyond 5G services in most of the considered scenarios. Only in extreme latency-critical scenarios, a small number of the cells might not fully satisfy the latency requirements of a low layer split option due to multiple microwave hops in the microwave-based architecture. © 2023 Optica Publishing Group

http://dx.doi.org/10.1364/JOCN.482865

1. INTRODUCTION

5G and beyond networks are expected to support services requiring ultra-high capacity, low latency, and high-reliability performance. Enhanced mobile broadband (eMBB) and ultra-reliable low latency communications (URLLC) are examples of two critical service categories in the 5G scenario. An eMBB service requires extremely high data rates, while a URLLC service has low latency and high-reliability requirements [1]. Designing and deploying a transport network meeting these service requirements is challenging, with several options to be carefully weighed against each other.

The first aspect to consider is the choice of the functional split option. Baseband processing can be virtualized using general-purpose servers at the cell site or data centers (DCs) deployed in more central locations. There are eight standardized split options. Among them, high layer split (HLS) and low layer split (LLS) are the most used. With HLS, most of the baseband processing is performed at the cell sites, which allows for relaxed latency and capacity requirements in the transport network (TN) [2, 3]. On the other hand, with LLS, baseband processing takes place at more central DC locations allowing for load balancing, sharing of processing capabilities among cell sites, and optimizing spectrum usage. However, an LLS option requires a high data rate and strict latency requirements in the TN [4]. The second aspect of evaluating while designing a TN relates to which technology to consider. The two most popular options are fiber and microwave. Fibers provide high capacity, but deploying them is expensive, especially in large geographical areas. On the other hand, placing microwave devices on already deployed towers is cheaper and faster. However, in some cases, the reach and capacity of microwave links might be limiting factors [5]. The third aspect to consider is the level of flexibility and reconfigurability of the TN. The more flexible and reconfigurable an architecture is, the easier it is for an operator to adapt to traffic

changes and accommodate new capacity levels over time without requiring any equipment upgrade. These benefits come with a higher deployment cost, i.e., a reconfigurable TN architecture is more expensive than a non-reconfigurable one.

All the options mentioned so far should be weighed against their total cost of ownership (TCO), latency, and reliability performance (in terms of connection availability) to identify, for a given scenario, the most suitable TN deployment [6, 7]. The TCO analysis of different technologies and the choice of the best functional split option have always gained interest from academia and industry. Some works focus on the TCO analysis of fiber and/or microwave architectures given a specific functional split option [8–12]. On the other hand, the works in [13, 14] investigate the TCO of different fiber and microwave architectures when the functional split option is varied. As of yet, there is no comprehensive framework that investigates the TCO, latency, and reliability performance of various technology and functional split options.

This paper fills this gap by proposing a comprehensive framework to evaluate the TCO, average latency, and connection availability performance of fiber- and microwave-based TN deployment suitable for 5G and beyond scenarios. We consider both HLS and LLS options and analyze the implications of using reconfigurable equipment. We select eMBB and URLLC as representative 5G services taking into account their capacity, latency, and reliability requirements. Regarding the scenarios, we rely on data derived from real network deployments in a city in South America from a large and non-incumbent mobile operator. We consider three geo-types (i.e., dense urban, urban, and suburban) with different area sizes, average link lengths, cell site densities, and capacity characteristics. To investigate the generality of our conclusions, we also perform a sensitivity analysis to understand better the impact of the microwave equipment and the fiber trenching costs on the TCO performance, as these costs may vary from operator to operator and from country to country. Our results show that microwave-based architectures have lower TCO in the considered scenarios compared to their fiber-based counterparts in most cases for operators deploying equipment to connect new cell sites. The TCO gain varies depending on the functional split option, the geo-type, and the cost of microwave equipment and fiber trenching. These latter cost values can vary depending on the country, and the labor and equipment cost an operator has to deal with. On the other hand, microwave- and fiber-based architectures meet the latency and the connection availability requirements of eMBB and URLLC services.

The rest of the paper is organized as follows. Section 2 reviews the existing state of the art on the topic. Section 3 presents the TN architectures considered in this work, while Section 4 introduces the TCO, latency, and availability models. Section 5 presents and discusses the TCO, latency, and availability performance of TN options under exam. Finally, conclusions are drawn in Section 6.

2. LITERATURE REVIEW

Mobile network operators are always keen to explore different deployment and technology options to contain the cost of their network deployments. For this reason, this topic has been extensively addressed in the literature.

The authors in [8] presented a TCO framework for evaluating the capacity and cost performance of a number of 5G deployment strategies. They assessed the cost savings of sharing infrastructure assets between two mobile network operators. However, they considered only a fiber-based infrastructure. The authors in [9] proposed a framework for economic viability analysis of 5G networks when fiber and microwave technologies are used to deploy the TN. Their results reveal that a low TCO solution does not always lead to high profits. Moreover, their results show the impact of choosing the right technology to maintain the economic benefits of heterogeneous network deployment. The work in [10] compares the TCO of a network deployment using a combination of wired and wireless backhaul technologies in three cities with different user densities. The results show that a microwave-based approach always offers lower TCO than a fiber-based. A more extensive TCO analysis is proposed in [11, 12], where the authors compared the deployment cost of wireless and fiber (point-to-point (PtP) and passive optical network (PON) options) transport technologies. The work in [11] focuses on the backhaul segment of a fixed-wireless access use case. In contrast, the authors in [12] considered a general 5G mobile network and the TCO implication of using an HLS option for the TN segment. Their results show that microwave gain depends on the cost of fiber deployment and microwave equipment. All the works mentioned so far focus on the backhaul or HLS option. On the other hand, it is important also to analyze the TCO performance of a TN using an LLS option in case an operator wants to adopt this solution. LLS is a more challenging option regarding capacity and latency requirements. Consequently, it requires the deployment of more expensive devices. The authors in [13, 14] presented a framework for the TCO analysis of a 5G TN considering various technologies (e.g., wireless, optical) and split options (i.e., LLS and HLS). The results in [13] are related to four 5G use cases and show that an HLS option has either higher or lower TCO than LLS, depending on the service under exam. The results in [14] demonstrate that using LLS and a hybrid composition of optical and wireless is a cost-efficient deployment solution.

All the literature works described so far looked only into the TCO performance of the different technological options for TNs. However, none of them looked into the latency, reliability, and reconfigurability performance of the architectures they examined. On the other hand, using specific devices and choosing a specific architecture may result in different latency and connection availability performances, not to mention the capability to adapt to traffic changes without requiring equipment upgrades. Considering these additional performance aspects is crucial because it might limit the applicability of a given TN solution or lead to a degradation of overall network performance. In this work, on the other hand, these aspects are all included in the TCO analysis.

3. NETWORK ARCHITECTURES

This section presents the network architectures considered in the study. We assume the TN architecture in Fig. 1 with access, pre-aggregation, and aggregation segments as defined by [15]. The pre-aggregation segment consists of passive distribution nodes (PDNs) organized in pre-aggregation rings. This segment is connected, on one side, to the backbone/core part of the network through metro aggregation (MA) nodes placed on the aggregation ring and, on the other side, to the access segment via fiber aggregation (FA) nodes. The MA and the FA nodes host the optical devices and the equipment for layer three processing and aggregation. DCs can potentially be located at both nodes to process the baseband functions. On the other hand, the PDNs

hosts only the passive optical equipment needed to interconnect the FA nodes to the pre-aggregation rings. We assume a non-incumbent operator who needs to get the right of using the fiber over pre-aggregation rings from the incumbent operator. In the access segment, the FA nodes are connected to macrocells (MCs) and/or small cells (SCs) using fiber and/or microwave. In the following, we present the microwave and fiber architectures of the access segment used to implement the HLS and LLS options in detail.

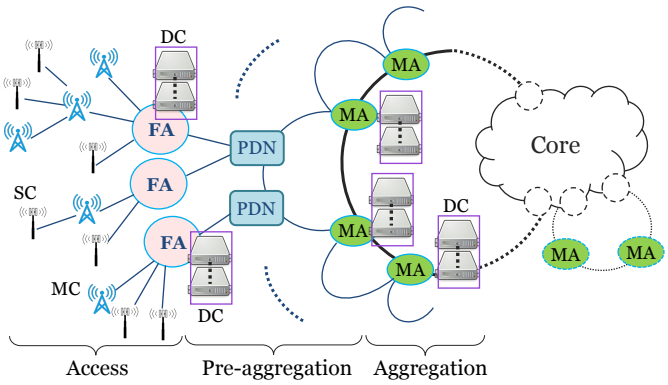

Fig. 1. Network architecture. Small cells (SCs) and macrocells (MCs) are connected to fiber aggregation (FA) nodes. Data centers (DCs) can be placed at the FA and metro aggregation (MA) nodes.

A. Architectures for High Layer Split

We assume a baseband functional split option 2 [3, 16] where most of the baseband functions are processed at the cell site, while the remaining functions are processed at the DCs connected to the MA nodes.

We consider two options for the HLS architecture, i.e., non-reconfigurable (*NR*) and reconfigurable (*R*). The *NR* and *R* pre-aggregation segments are shown in Fig. 2. In both architectures, each DC is connected through a router to its MA node, which, in turn, is connected to the pre-aggregation ring using optical transceivers (Tx/Rxs) and multiplexer (MUX)/de-multiplexers (DeMUXs) devices. In the *NR* architecture, colored transceivers and non-reconfigurable multiplexers (MUX-NR) are used at the MA nodes, while passive optical add-drop multiplexer (OADM) devices are used at FA nodes to add/drop wavelengths to/from the pre-aggregation ring. On the other hand, the *R* architecture uses reconfigurable multiplexers (MUX-R) with advanced features and reconfigurable optical add-drop multiplexers (ROADMs). The colored wavelengths dropped at the ROADM are converted to grey traffic using transponders and delivered to grey Tx/Rx.

We consider three options for the access segment (Fig. 3), all compatible with both an *R* and an *NR* pre-aggregation segment. In the first case, we have PtP optical fiber connections with traffic aggregation at the networking device (ND) ($H^F_{NR,1}$ and $H^F_{R,1}$), in the second a PON-like architecture ($H^F_{NR,2}$ and $H^F_{R,2}$) [17], and in the third case a tree-based architecture (H^{MW}_{NR} and H^{MW}_{R}) using microwave and mmWave band devices. In the PtP case, the traffic is carried from the FA to MCs/SCs over dedicated fibers. In the PON-like architecture, the traffic from the FA is multiplexed over a feeder segment and then split towards all MCs/SCs connected to the FA node. Each MC/SC filters out the wavelength addressed to it. As shown in the figure, we can also have MCs and/or SCs directly connected to the FA. In the tree-based microwave case, the traffic is sent over a feeder link to a feeder node using microwave and mmWave band devices, which is connected by a wireless link to MCs/SCs. The microwave equipment (i.e., a main component in the feeder node) includes a microwave indoor unit that performs ND functionalities. The NDs at an FA node performs link/network layer processing and traffic grooming. The ND at a cell site has the same traffic aggregation functionality as the cell site router defined in O-RAN [15]. For the sake of simplicity, the required servers for baseband processing at the MCs/SCs are not shown in Fig. 3.

In the considered architectures, the path from the cell site to the FA is not protected by a backup path to reduce the cost. However, the path from FA to MA is protected using a backup path since it serves multiple sites. The protection switching between these two paths is managed by the ND at the FA (shown in Fig. 3).

B. Architectures for Low Layer Split

For LLS, we assume the split option is 7.2x [4]. With this option, a small portion of the baseband processing is done at the MCs/SCs while most of the baseband processing is performed at the DCs placed, in our case, at the FA node, and connected to the cell sites through a router at the FA. Given the demanding requirements of LLS in terms of bandwidth and latency, baseband processing at the MA is not practical. There are two main reasons for this choice: (i) it is expensive to carry a large amount of data to the MA and (ii) the distances between the FA and the MA might have a non-negligible impact on the overall latency performance.

We consider four architectural alternatives (Fig. 4). For the sake of simplicity, the required servers for baseband processing at the MCs/SCs are not shown in Fig. 4. The first architecture (L^F_1) is based on PtP optical fiber links. The traffic addressed to each cell sector is sent from the DC at the FA to the respective MCs/SCs over dedicated fiber cables. The second architecture (L^F_2) is an evolution of the L^F_1 where traffic aggregation takes place at the ND, thus allowing to save on the fiber cost. In both L^F_1 and L^F_2, we use only grey Tx/Rxs. The third architecture (L^F_3) has a PON-like topology. The traffic for the MCs/SCs is multiplexed at the FA using MUX and colored transceivers, then split towards cell sites using a power splitter. Some other MCs/SCs are connected to the FA without any power splitter or MUX, and they use grey Tx/Rx. The fourth architecture is microwave-based (L^{MW}). It uses microwave and mmWave band components to connect the FA to the MCs/SCs. We consider two cases depending on the amount of traffic carried over a feeder link. We use a single microwave or mmWave band device if the traffic over the feeder link is not larger than the capacity of an existing device (i.e., as in the left side of L^{MW} figure). Otherwise, we connect the FA to the feeder node with a fiber link (i.e., as in the right side of L^{MW} figure). The ND at the feeder node aggregates traffic from different sites and sends it to the FA. Table 1 is a list of all considered architectures.

The architectural options described so far use components with different capacities, costs, and capabilities, resulting in different cost, latency, and availability performances. We describe the models used to assess these performance metrics in the following.

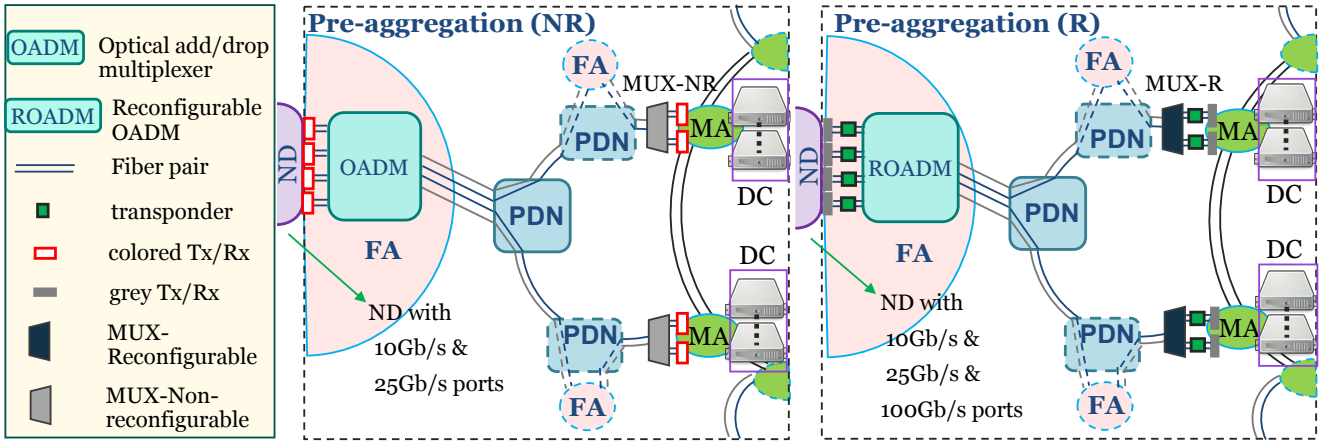

Fig. 2. Pre-aggregation segment: high layer split (HLS) option deployment. Non-reconfigurable (*NR*) and reconfigurable (*R*) options.

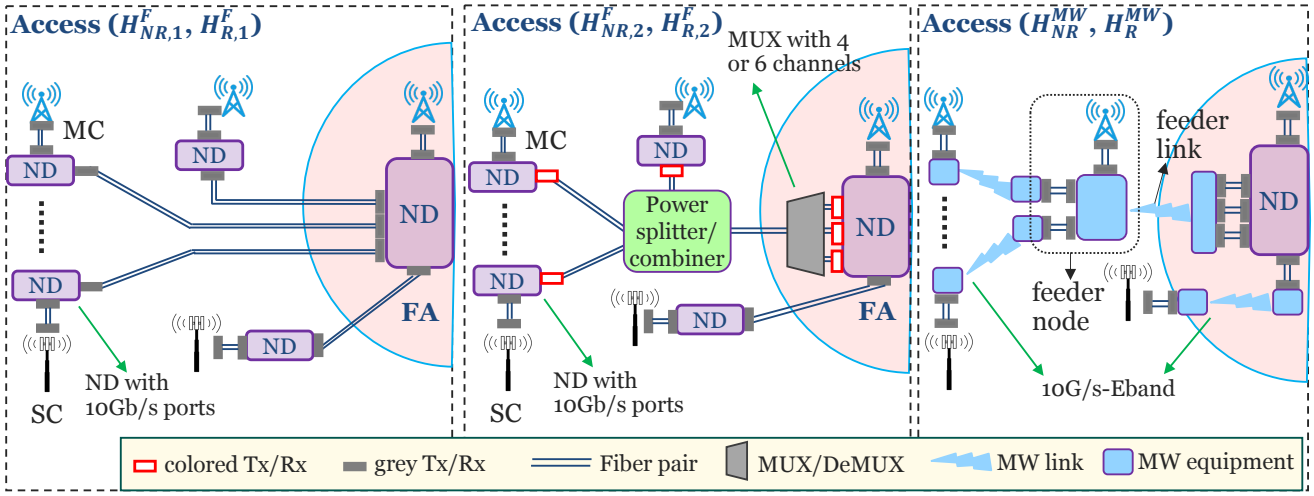

Fig. 3. Access segment: fiber- [($H^F_{NR,1}$, $H^F_{R,1}$),($H^F_{NR,2}$, $H^F_{R,2}$)] and microwaved-based (H^{MW}_{NR}, H^{MW}_{R}) architectures for high layer split (HLS) option. The pre-aggregation segment is the same in all three cases. Small cells (SCs) and macrocells (MCs) send traffic to networking devices (NDs) at the fiber aggregation (FA) node.

Table 1. List of considered architectures. Agg. refers to aggregation at the cell site.

High layer split		Low layer split
Non-reconfigurable	Reconfigurable	microwave: L^{MW}
microwave: H^{MW}_{NR}	microwave: H^{MW}_{R}	fiber-PtP: L^F_1
fiber-PtP-Agg.: $H^F_{NR,1}$	fiber-PtP-Agg.: $H^F_{R,1}$	fiber-PtP-Agg.: L^F_2
fiber-PON: $H^F_{NR,2}$	fiber-PON: $H^F_{R,2}$	fiber-PON: L^F_3

4. TCO, LATENCY, AND AVAILABILITY MODELING

In this section, we present the models used to assess the TCO, latency, and availability performance of the architectures examined in this study.

A. TCO modeling

We compute the value of the capital expenditure (CapEx) as the sum of the cost of the components deployed in fiber- and microwave-based architectures:

$$CapEx = Ac_{\text{opt}} + Ac_{\text{MW}} + Ac_{\text{fib}} + PA_{\text{fib}} + PA_{\text{opt}} + Comp, \quad (1)$$

where:

$$Ac_{\text{opt}} = \sum C_{\text{Tx/Rx}} + \sum C_{\text{MUX}} + \sum C_{\text{splitter}} + \sum C_{\text{FA router port}} + \sum C_{\text{ND}}, \quad (2)$$

$$Ac_{\text{MW}} = \sum C_{\text{MW}}, \quad (3)$$

$$Ac_{\text{fib}} = \sum_{(i,j)\in\mathcal{N}_A} \mu_{(i,j)} \times d_{(i,j)} \times FDC \times \left(C_{\text{trenching}} + C_{\text{fiber cables}}\right), \quad (4)$$

$$PA_{\text{fib}} = \sum_{(i,j)\in\mathcal{N}_{FP}} \left(\mu_{(i,j)} \times d_{(i,j)} \times FDC \times \left(C_{\text{trenching}} + C_{\text{fiber cables}}\right)\right) + \sum_{(i,j)\in\mathcal{N}_{PP}} \left(\mu_{(i,j)} \times d_{(i,j)} \times f_{(i,j)} \times C_{\text{IRU fiber}}\right), \quad (5)$$

$$PA_{\text{opt}} = \sum C_{\text{Tx/Rx}} + \sum C_{\text{MUX}} + \sum C_{\text{transponder}} + \sum C_{\text{OADM/ROADM}} + \sum C_{\text{MA router port}}. \quad (6)$$

Ac_{opt} is the cost of all devices used in the access segment, including all the Tx/Rx pairs, MUXs, power splitters, router

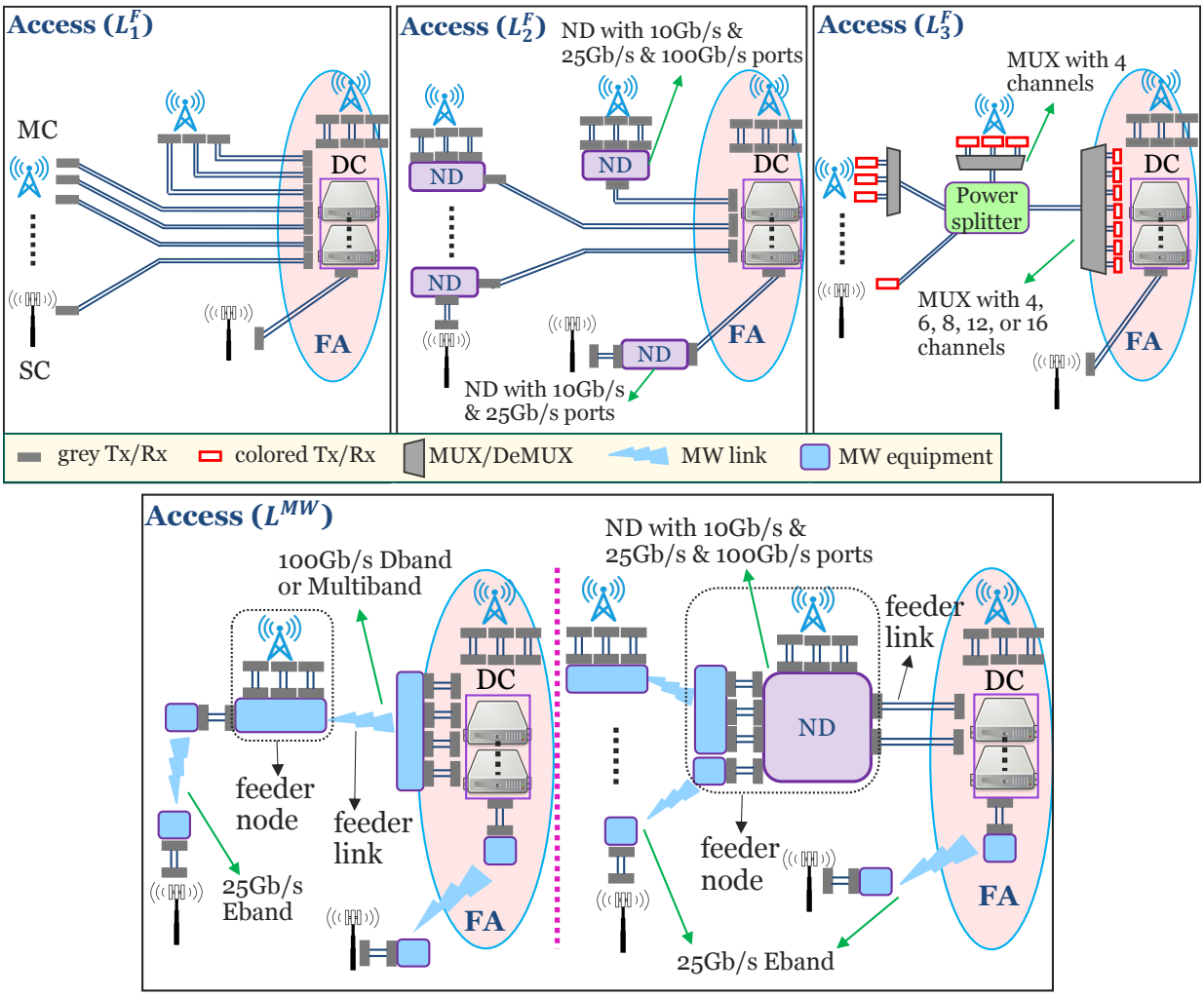

Fig. 4. Access segment when considering a low layer split (LLS) option: fiber- (L_1^F, L_2^F, L_3^F) and microwave-based (L^{MW}) architectures. Small cells (SCs) and macrocells (MCs) send their traffic to the data center (DC) at the fiber aggregation (FA) node.

ports at FA, and ND. Depending on the architecture under exam, some of these costs equal zero. To account for the cost of the router ports at FA ($C_{\text{FA router port}}$), we consider a linear model in which $C_{\text{FA router port}}$ is computed as the product of the required router ports and the cost of using one. Ac_{MW} is the cost of all the microwave devices (C_{MW}) in the network. Ac_{fib} is the fiber deployment cost in the access segment. We consider all the possible node couples (i, j) in the access segment, i.e., $\mathcal{N}_A$. If two nodes are connected by a fiber link ($\mu_{(i,j)} = 1$), their cost contribution is a function of the cost of fiber cables (i.e., $C_{\text{fiber cables}}$, which depends on the number of fibers deployed between the two nodes) and the fiber trenching cost ($C_{\text{trenching}}$) per unit of distance (e.g., [km]). The Euclidean distance between i and j ($d_{(i,j)}$) is multiplied by the fiber deployment conversion (FDC) factor to account for obstacles on the fiber deployment route. If two nodes are not connected by a fiber link, $\mu_{(i,j)} = 0$. PA_{fib} is the cost of deploying and right of use of fibers in the pre-aggregation segments. We split this cost into two parts. The first one is associated with fiber cables deployed to connect the FA to the PDN, where trenching is needed. The same rationale used to compute Ac_{fib} applies here, where $\mathcal{N}_{FP}$ refers to the set of all FA and PDN node couples (i, j) in the pre-aggregation segment. The second part is associated with the indefeasible right of use (IRU) cost for the fibers on the pre-aggregation rings. As explained in Section 3, we assume a non-incumbent operator that does not own fiber over the pre-aggregation rings. $C_{\text{IRU fiber}}$ is a one-time, upfront cost for the right to use a fiber pair per unit of distance (e.g., [m]) for a specific duration of time (i.e., usually 15, 20, or 30 years). Set $\mathcal{N}_{PP}$ includes all the PDN node couples (i, j) and $f_{(i,j)}$ is the number of required fiber pairs between (i, j). $\mu_{(i,j)}$ is equal to one if nodes i and j are connected, zero otherwise. PA_{opt} is the cost of all the devices in the pre-aggregation segment, including all the Tx/Rx pairs, MUXs, transponders, OADMs/ROADMs, and router ports at the MA. Similar to $C_{\text{FA router port}}$, to account for the cost of the router ports at MA, we consider a linear model in which $C_{\text{MA router port}}$ is computed as the product of the required ports and the cost of using one. The router ports on the MA/FA nodes are the endpoints of the transport network, where we plug in Tx/Rxs. Finally, $Comp$ is the cost of all the computing resources (i.e., servers) located at the MCs/SCs and DCs for baseband processing.

The operational expenditure (OpEx) during one year of operations is assumed to be proportional to the CapEx [8] and energy

consumption cost and it is defined as:

$$OpEx = \eta_1 \times (Ac_{\text{opt}} + PA_{\text{opt}} + Comp) + \eta_2 \times (Ac_{\text{MW}} + Ac_{\text{fib}} + PA_{\text{fib}}) + m \times C_{\text{license}} + E_{\text{MW}} + E_{\text{ND}} + E_{\text{ROADM}} + E_{\text{MUX-R}} + E_{\text{transponder}} + E_{\text{server}}, \quad (7)$$

where η_1 and η_2 are multiplicative factors. They are not the same because we assume different operation and maintenance cost values for microwave and fiber compared to the optical devices and servers. C_{license} is the licensing fee to use the microwave frequencies, and m is the total number of microwave links. E_{MW}, E_{ND}, E_{ROADM}, $E_{\text{MUX-R}}$, $E_{\text{transponder}}$, and E_{server} refer to energy consumption cost of all the active components in the considered architectures, i.e., microwave devices, NDs, ROADMs, reconfigurable MUXs, transponders, and servers, respectively. The contribution of energy consumption of Tx/Rxs is neglected as it is small and negligible compared to that of other equipment. E_{x}, for a component x, is obtained by multiplying the power consumption of x, the number of x components in a given architecture, and the mean energy price.

B. Latency modeling

For latency evaluation, we consider two of the main service categories in the 5G networks, i.e., eMBB and URLLC [1].

Different functional split options have different transport latency requirements [2, 18]. Finding a unique definition for the latency requirement when looking at the works in the literature is not straightforward. The O-RAN alliance introduced different latency requirements for the TN [19]. We consider their recommendations as the target latency requirement for the LLS architectures. On the other hand, the HLS option is the main focus of ITU. They recommended user plane (UP) latency requirements of the eMBB and URLLC services, including both radio and TN domains [20]. Therefore, we consider UP latency as the target key performance indicator for the HLS architectures.

The value of UP latency in the case of an HLS option (l_{HLS}) and of the transport latency over the fronthaul in the case of an LLS option (l_{LLS}) are computed as [19–21]:

$$l_{\text{HLS}} = l_{\text{UE}} + l_{\text{OTA}} + l_{\text{BBU}} + l^{\text{MW}}_{\text{prop}} + l^{\text{fiber}}_{\text{prop}} + l_{\text{ND}} \times n_{\text{ND}}, \quad (8)$$

$$l_{\text{LLS}} = l^{\text{MW}}_{\text{prop}} + l^{\text{fiber}}_{\text{prop}} + l_{\text{ND}} \times n_{\text{ND}}, \quad (9)$$

where l_{UE}, l_{OTA}, and l_{BBU} are the latency contributions due to the user equipment (UE), the over-the-air (OTA) propagation between a user and the cell site, and the baseband unit (BBU) processing, respectively. $l^{\text{MW}}_{\text{prop}}$ and $l^{\text{fiber}}_{\text{prop}}$ refer to the propagation delay over the microwave and fiber links, respectively. l_{ND} is the switching latency introduced by each ND, and n_{ND} is the number of ND on the route from an MC/SC to the DC where their baseband processing takes place.

C. Availability modeling

We aim to calculate the connection availability between any cell site and its corresponding DC. We concentrate on the segment between the cell site and the FA since the path from the FA to the MA is protected, as explained in Section 3, and its impact on overall unavailability is negligible.

A connection between a cell site and the FA may not always be up because any of the elements along the path (e.g., Tx/Rx, ND, power splitter/combiner, MUX/DeMUX, transponder, OADM/ROADM, microwave links, and fiber cables) may fail. We include all these elements in the unavailability calculation. Unavailability is defined as the probability that the system or a component is down at an arbitrary point in time. The intuition behind connection unavailability calculation is to consider the product or summation of the unavailability of elements on the path depending on whether they are connected in parallel or series, respectively. Let's consider $H^F_{NR,1}$ as an example. Starting from an MC, the connection unavailability is the sum of the unavailability of the elements that are not protected (the Tx/Rx and the ND at the MC location, the Tx/Rxs and fiber cables between two NDs, the ND at the FA location, and the OADM) plus the multiplication of unavailability of elements that are protected (colored Tx/Rxs plugged into the ND).

The general connection availability model of any cell site in the network is defined as [21, 22]:

$$A_{\text{conn}} = 1 - UA_{\text{conn}} = 1 - \left(\sum_{i \in \mathcal{NP}} UA_i + \sum_{(j,k) \in \mathcal{P}} UA_j \times UA_k \right), \quad (10)$$

$$UA_i = \frac{MTTR_i}{MTBF_i} = \frac{MTTR_i}{MTTR_i + MTTF_i}. \quad (11)$$

UA_{conn} represents the connection unavailability from a given SC/MC to its corresponding DC. UA_i represents the unavailability of the element i. An element belongs to the protected set ($\mathcal{P}$) if at least one counterpart can take over as backup in case of failure. Otherwise, the element belongs to the unprotected set ($\mathcal{NP}$).

In Eq. (11), $MTTR_i$ is the mean time to repair (MTTR) of element i, which includes the time for detecting a fault, making a diagnosis, and dispatching the field force to restore the service. $MTTR_i$ is independent of the faulty element involved but mainly depends on the distance between the site and the warehouse and procedures followed by operation/maintenance teams for troubleshooting and replacement tasks. $MTBF_i$ is the mean time between failures of element i. Finally, $MTTF_i$ is the mean time to failure (MTTF) of element i during which the element is up and running.

In the next section, we use the models for TCO, latency, and availability to quantitatively analyze the performance of the considered architectures in HLS and LLS.

5. PERFORMANCE EVALUATION AND DISCUSSION

In this section, we first present the assumptions on the network topology. Then, we show the results for TCO, average latency, and availability performance relative to the architectures presented in Section 3 for HLS and LLS. To this aim, we developed a custom Python-based framework that mimics the deployment of the architectures in different scenarios and returns the values of the performance metrics.

A. Network dimension and assumptions

We consider three geo-types, i.e., dense urban, urban, and suburban. Each geo-type has a different area size, average link length, density of MCs and SCs, and capacity of an MC/SC. The number of MCs, SCs, FAs, and PDNs and the distances among them are summarized in Table 2. These values are derived from mobile network deployments by a large, non-incumbent operator in a city in South America. They were obtained via conversation with a system vendor.

Table 2. Network topology parameters. $d_{(i,j)}$ is the Euclidean distance between nodes i and j in [m], and R_{peak} and R_{avg} are in [Gb/s] [16, 19, 23]. MC/SC-x-hop is the number of MCs/SCs that are x hops away from the FA.

	dense urban	urban	sub-urban		dense urban	urban	sub-urban		dense urban	urban	sub-urban
R_{peak}- SC- HLS	10	10	10	$d_{(PDN,PDN)}$	799	1098	1750	#FA	214	273	119
R_{avg}- SC- HLS	3	3	3	$d_{(FA,PDN)}$	250	350	450	#SC-1-hop	1316	476	34
R_{peak}- MC- HLS	10	10	5	$d_{(MC,MC/FA)}$	400	600	1000	#SC-2-hop	304	317	83
R_{avg}- MC- HLS	10	10	5	$d_{(SC,MC/FA)}$	100	200	400	#MC-0-hop	214	273	119
R_{peak}- SC- LLS	25	25	25	#MA	14	10	7	#MC-1-hop	109	275	142
R_{avg}- SC- LLS	25	25	25	#PDN / pre-agg. ring	5	6	7	#MC-2-hop	22	99	91
R_{peak}- MC- LLS	75	75	75	#FA / pre-agg. ring	12	14	16	max. #sites on feeder	5	5	6
R_{avg}- MC- LLS	75	75	75	#aggregation ring	2	2	1				

For designing the network shown in Fig. 1, we start by connecting the MAs on the aggregation ring. Then, we compute the number of required pre-aggregation rings as the ratio between the total number of FAs and the number of FAs per pre-aggregation ring (rounded up to the next integer) (Table 2). We put the PDNs on the pre-aggregation rings, then connect the FAs to the PDNs. Finally, we connect the MCs and SCs to the FAs. In the table, MC/SC-x-hop represents the number of MCs/SCs that are x hops away from the FA.

The aggregated traffic over a feeder link or an FA-PDN link is computed as $R_{agg}(N) = \max\left(R_{peak}, N \times R_{avg}\right)$ [16, 19], where R_{peak} is the peak rate of an MC/SC at quiet times (i.e., when the cell serves the lowest number of users), R_{avg} is the average rate of an MC/SC during busy hours, and N is the number of MCs and SCs sending traffic over a feeder link or an FA-PDN link. The values of R_{peak} and R_{avg} for an MC/SC are shown in Table 2.

We rely on the values in Table 3 for the TCO and availability evaluation. The table shows the MTTF and cost values for microwave and mmWave devices, optical components, NDs, router ports on MA/FA, and computing servers. The cost of a component is given in cost units [CU], which corresponds to the cost of a 10 [Gb/s] grey transceiver. The table also shows the power consumption of active components in power consumption units [PCU], which corresponds to the power consumption of one transponder. The values in Table 3 are obtained from a single microwave and an optical vendor inventory. We assume that the cost of fiber cables ($C_{\text{fiber cables}}$) depends on the number of required fibers in a duct and is obtained from Table 1 in [24]. The cost values of the microwave and mmWave components are per microwave link and are different depending on their features and capabilities (e.g., maximum capacity, maximum reach, used technology). When selecting among the options in Table 3 for a given equipment (e.g., microwave device, NDs, MUXs, and Tx/Rx), we choose the option with the lowest cost that meets a given set of requirements (e.g., capacity, reach, number of ports, and/or number of channels).

We assume the transmission rates of colored Tx/Rx, transponder, and grey Tx/Rx (Fig. 2) to be 25 [Gb/s], 100 [Gb/s], and 100 [Gb/s], respectively. In Fig. 3, all Tx/Rxs are 10 [Gb/s]. In Fig. 4, all Tx/Rxs are 25 [Gb/s] except the ones that are connecting the DC to the NDs located at the MC sites and feeder nodes, which are 100 [Gb/s].

The cost of a router port (25 [Gb/s] and 100 [Gb/s]) in Table 3 is based on the assumption that one router in a data center may not exclusively be used for 5G TN, but it can be exploited/shared by different services/customers/operators. Thus, to compute the average cost of one port, we uniformly spread the total cost of the router over the number of its ports.

To connect an SC to an MC/FA, the FDC factor of 1.5, 1.4, and 1.3, is assumed for dense urban, urban, and sub-urban geo-types, respectively. These values change slightly when we connect an MC to an MC/FA, i.e., the FDC factors become 1.2, 1.1, and 1.

In *NR* architectures, we assume a maximum number of OADMs connected via the same fiber pair and over the same pre-aggregation ring equal to 5. This is to avoid violating the signal quality threshold required over the pre-aggregation ring due to the signal loss introduced by a larger number of OADMs. To compute this value, we considered the insertion loss caused by the components along the path from the FA to the MA (i.e., OADMs, connectors on PDNs, and fiber), the launch power of the transmitter, and the receiver sensitivity. However, we do not have this constraint in the *R* architectures, thanks to the lower loss introduced by the ROADMs. The ROADMs cost in Table 3 includes the cost of optical amplification. Depending on the amount of traffic over a pre-aggregation ring, more than one fiber pair might be needed on that ring.

We assume that placing computing servers for baseband processing at the MA leads to a 15% and 50% reduction of the CapEx and OpEx of the computing resources, respectively [10], compared to when computing servers are located at the cell site. We assume that these reductions become 7.5% and 25% when baseband processing units are deployed in the DC at the FA. These savings come from the benefits of centralized processing. In centralized processing, the operators can benefit from the economy-of-scale of large DCs. In addition, resource utilization can be improved as centralized processing enables the dynamic sharing of resources, which reduces OpEx [25]. The amount of CPU cores required for baseband processing is assumed to be as in [26].

To compute OpEx as a percentage of CapEx, we assume microwave equipment and fiber cable are easier to maintain over time than other equipment and computing servers. As a result, $\eta_1 = 15\%$, and $\eta_2 = 5\%$. C_{license} is assumed to be 17.2 [CU] per microwave link. The mean energy price is assumed to be 0.00026 [CU/(PCU×h)] [27]. The TCO is computed over 5 years

Table 3. Ranges for the components' cost, MTTF, and power consumption values. The component cost is expressed in cost unit [CU], except for the IRU and fiber trenching costs measured in [CU/m]. The cost of fiber cables (in [CU/fiber/km]) is obtained from Tab.1 [24], which depends on the number of fibers per cable. The MTTF is expressed in years. PW refers to power consumption measured in power consumption unit [PCU].

microwave Component	cost	MTTF	PW	Component	cost	MTTF	Component	cost	MTTF	PW	Component	cost	MTTF
10Gb/s-Eband				MUX (4CH)			ND: (8×10Gb/s)				IRU fiber	0.1	
25Gb/s-Eband				MUX (6CH)	69.8	460	ND: (6×10Gb/s				fiber trenching	2.4	
50Gb/s-Dband	153	15	1.6	MUX (8CH)	to	to	4×(10/25Gb/s))	114.8		2.7	port on router		
50Gb/s-Eband	to	to	to	MUX (12CH)	119.7	950	ND: (8×10Gb/s	to	30	to	25Gb/s	95.7	
75Gb/s-Multiband	918.6	25	6.1	MUX (16CH)			10×(10/25Gb/s)	267.9		5.3	100Gb/s	153.1	
100Gb/s-Dband				MUX-NR (40CH)			2×100Gb/s)				Tx/Rx		
100Gb/s-Multiband				OADM (4CH)			ND: (20×10Gb/s				grey 10Gb/s		
				power splitter	19	484	8×(10/25Gb/s)				grey 25Gb/s	1	228
				2 fibers			2×100Gb/s)				grey 100Gb/s	to	to
				8 fibers	6		transponder	434.5	38	1	colored 10Gb/s	29.3	543
				12 fibers	to	275.1	MUX-R (40CH)	to	to	to	colored 25Gb/s		
				24 fibers	1.1		ROADM (8CH)	1206.9	75	2.4			
				48 fibers			server (8 cores)	127.6		6.6			

of operations. We evaluate different architectures introduced in Table 1 in Section 3.

B. HLS: TCO analysis

Figure 5 presents the TCO breakdown for the HLS architectures (Fig. 2 and 3), computed using Eq. (1). In the considered geo-types, H_{NR}^{MW} has lower TCO compared to $H_{NR,1}^{F}$ and $H_{NR,2}^{F}$. In the access segment, the sum of the microwave and optical devices costs ($Ac_{\text{MW}} + Ac_{\text{opt}}$) in H_{NR}^{MW} is lower than the sum of the fiber deployment and optical devices ($Ac_{\text{fib}} + Ac_{\text{opt}}$) costs in $H_{NR,1}^{F}$ and $H_{NR,2}^{F}$. The pre-aggregation segments are the same for all NR architectures, thus, $Comp$, PA_{opt}, and PA_{fib} are the same. The TCO gain of H_{NR}^{MW} is different depending on the geo-type. H_{NR}^{MW} has a larger TCO gain in urban and sub-urban areas where links are, on average longer than in dense urban ones, which leads to a higher cost of fiber deployment in the access segment (Ac_{fib}). Also, Fig. 5 shows that $H_{NR,1}^{F}$ and $H_{NR,2}^{F}$ have almost similar TCO values.

When looking at the performance of H_{R}^{MW} versus $H_{R,1}^{F}$ and $H_{R,2}^{F}$, we observe similar trends as with their non-reconfigurable counterparts, with the only difference that in absolute terms their TCO value is higher. This is due to the higher cost of the ROADMs, 100 [Gb/s] Tx/Rx, and 100 [Gb/s] transponders. On the other hand, a reconfigurable architecture provides larger capacity and more flexibility in the pre-aggregation segment.

We performed a sensitivity analysis of the cost of fiber trenching and microwave devices. These values can differ depending on the country/operator (e.g., because of lower/higher labor costs) and the ability to negotiate good prices. Figure 6 shows the TCO as a function of fiber trenching cost varied between ±60% of our benchmark (i.e., 2.4 [CU/m]) for different discount levels for the microwave devices, i.e., ±20% of our benchmark (BM) values in Table 3. The gain of using H_{NR}^{MW} in urban and sub-urban geo-types is not affected very much by the varying price of the microwave devices. On the other hand, in dense urban areas, the gain of H_{NR}^{MW} is affected more. The TCO of H_{NR}^{MW} is slightly affected by variation in fiber trenching cost because we need to deploy fiber between the FA and the PDN. A similar sensitivity analysis was performed for the reconfigurable architecture case, but it is not reported here because of space constraints. The trend is similar to the ones presented in Fig. 6.

Table 4. Latency requirements and contributing values for considered services in [ms] [19, 20, 28–30].

	latency requirements		latency values			
	L_{HLS}	L_{LLS}	l_{OTA}	l_{BBU}	$l_{\text{prop}}^{\text{MW}}$	l_{ND}
eMBB	4	0.1	0.5	1	0.02	0.01
URLLC-T	1	0.05	0.125	0.2	0.02	0.01
URLLC-S	0.5	0.025	0.125	0.2	0.02	0.01

C. HLS: latency performance evaluation

To evaluate the latency performance of the architectures presented in this study, we consider two families of services, i.e., eMBB and URLLC (including URLLC-latency-tolerant (URLLC-T) and URLLC-latency-sensitive (URLLC-S)). Their latency requirements (L_{HLS} and L_{LLS}) and the values of latency contributors (l_{BBU}, l_{OTA}, $l_{\text{prop}}^{\text{MW}}$, and l_{ND}) for each type of service are shown in Table 4. We assume that l_{BBU} and l_{OTA} are different for eMBB and URLLC services [29–31]. We set $l_{\text{UE}} = 0$ while $l_{\text{prop}}^{\text{fiber}}$ is computed as the ratio between the distance traversed and the speed of light propagating into the fiber (v=2×10^8 [m/s]). Finally, we define the average latency performance metric as:

$$P(L) = \frac{\#\text{sites with } l \leq L}{\text{total \#of sites}} \times 100, \quad \textbf{(12)}$$

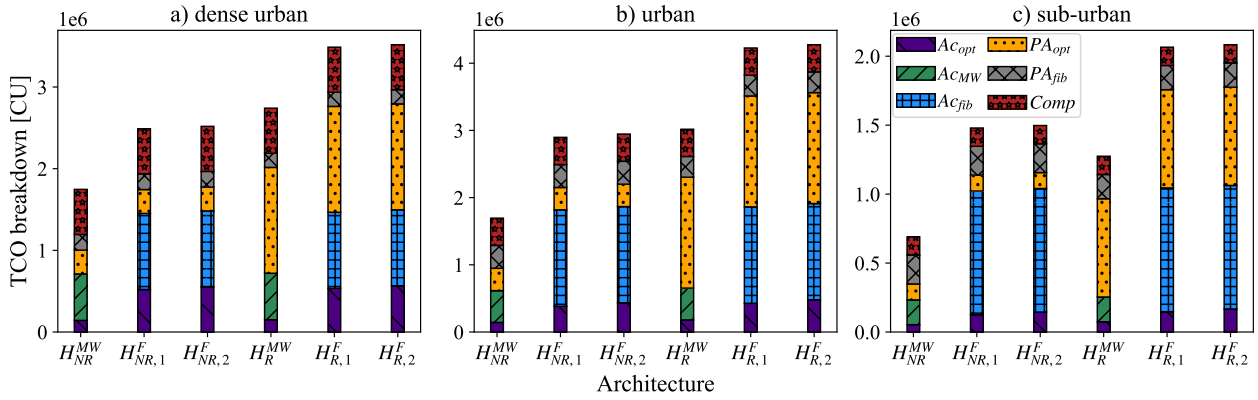

Fig. 5. HLS option: TCO breakdown for Reconfigurable (R) and Non-Reconfigurable (NR) architectures for different geo-types.

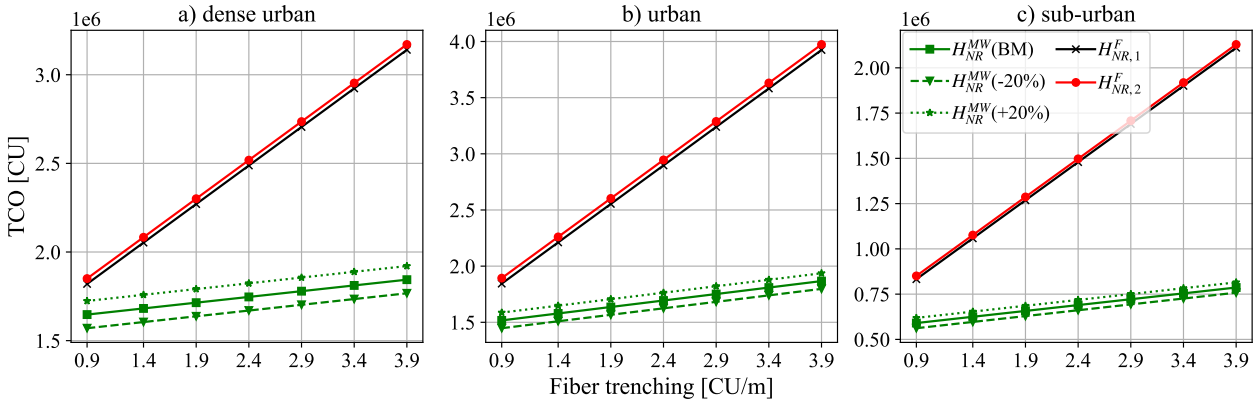

Fig. 6. HLS option: TCO variations while changing the fiber trenching and microwave equipment cost.

where, l is computed as in Eq. (8). $P(L)$ measures, for a given latency requirement value L, what is the percentage of cell sites able to meet this requirement, i.e., $l_{\text{HLS}} \leq L$.

Figure 7 shows the average latency performance of the HLS architectures when provisioning an eMBB service. We observe that all MCs and SCs can meet the 4 [ms] eMBB requirement [20]. The range of latency variation over the whole network is small. The microwave- and fiber-based architectures have almost the same average latency performance because, in our analysis, the main contributors to latency are l_{BBU} and l_{OTA} which are transport technology independent. The R and NR architectures follow almost the same trends. The difference is due to the constraint on the maximum number of OADMs (i.e., 5) that can be used on the same fiber over a pre-aggregation ring in an NR architecture. Imposing this limitation leads to shorter fiber on pre-aggregation rings.

Figure 8 shows the average latency performance of the HLS architectures when provisioning URLLC services. The latency requirement for URLLC-T (i.e., 1 [ms] [20]) can be met by cell sites in all geo-types. The range of latency variation is small, and microwave- and fiber-based architectures have almost similar performance. URLLC-S services have, on the other hand, a more stringent latency requirement (i.e., 0.5 [ms]). In this case, if H^{MW}_{R} is used in a sub-urban area, 10% of the sites cannot meet this requirement. This is an extreme scenario where the penetration of this type of service is not very high. An operator can easily avoid this problem by covering these specific users with cell sites with acceptable average latency performance.

D. HLS: availability evaluation

Different parameters affect the connection availability in the microwave- and fiber-based TN architectures as explained in Section 4. In the fiber-based case, the fiber cable failure is due to fiber cuts and physical damage that can happen, for example, during construction works in the area. With microwave technology, we distinguish between two contributors to link unavailability, i.e., radio link failure and hardware failure. Radio link failure depends on electromagnetic propagation conditions/impairments. Microwave links are affected mostly by multipath and rain fading phenomena which can reduce the received signal level down to the system threshold and cause a temporary out-of-service of the radio connection. Microwave links are designed to meet a minimum availability target of 99.999% due to electromagnetic propagation. This value is set by ITU [32–34]. The unavailability of microwave hardware equipment can be expressed using its MTTR and MTTF values and Eq. (11).

We define a metric called average availability performance ($P(A)$) as the percentage of MCs and SCs with a value of connection availability, i.e., computed as in Eq. (10) not lower than A:

$$P(A) = \frac{\#\text{sites with } A_{\text{conn}} \geq A}{\text{total \#of sites}} \times 100. \quad \textbf{(13)}$$

While computing the value of A_{conn}, we utilize the values of $MTTF_i$ in Table 3 and assume that $MTTR_i$ is 4 hours [h] for all the devices (i.e., the value obtained through conversations with a system-vendor) except for fiber cable which is assumed

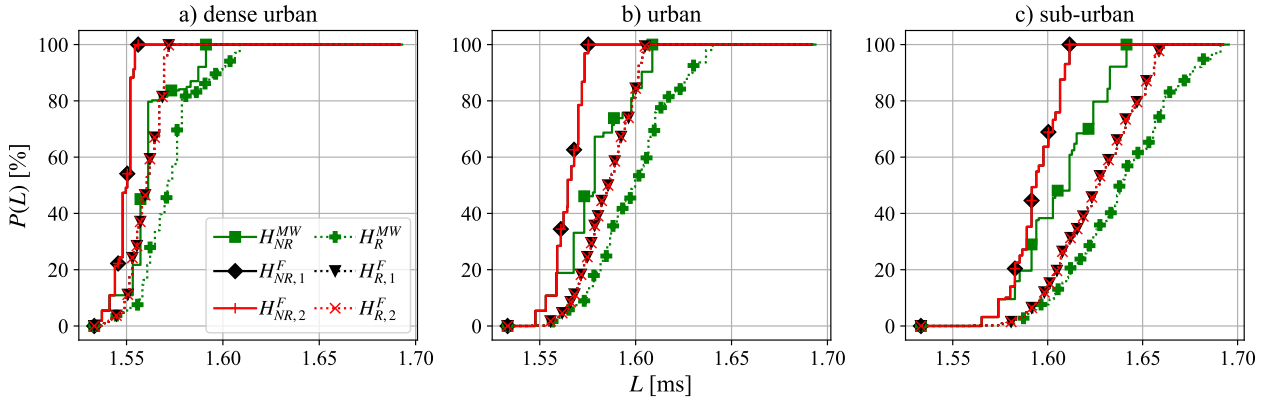

Fig. 7. HLS with eMBB service: average latency performance.

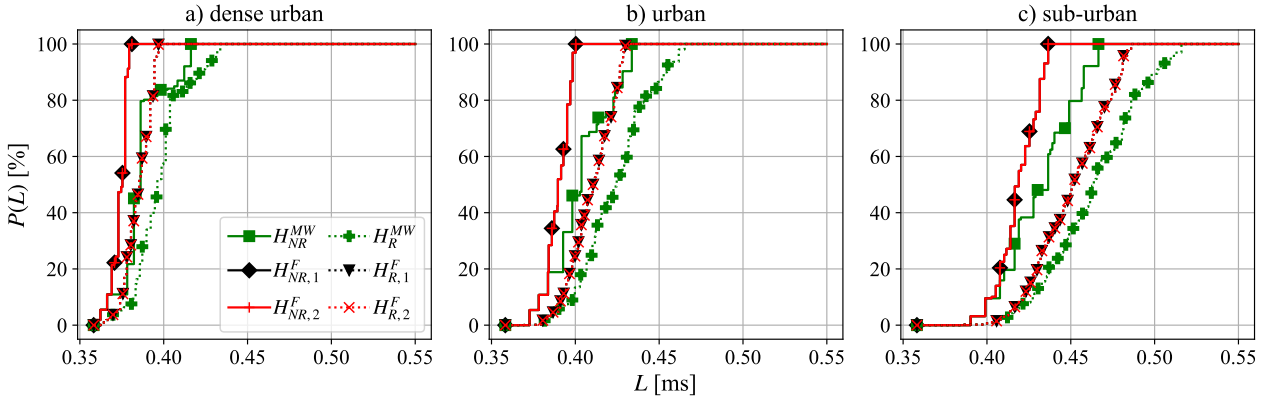

Fig. 8. HLS with URLLC service: average latency performance.

to be 24 [h] [22]. The value of UA_i for a fiber refers to 1 [km] and it should be multiplied by the length of the fiber cable that inter-connects two components.

Figure 9 shows the average availability performance of the HLS architectures. According to 3GPP, the connection availability of a TN should be in the [0.999,0.9999999] range [35]. Note that the connection availability used in this work is referred to as reliability in the 3GPP document [35]. All fiber- and microwave-based HLS architectures can provide connection availability values higher than 0.9999 (i.e., well within the 3GPP requirements) while connection availability up to 0.99998 can be provided by only a percentage of sites.

E. LLS: TCO analysis

Figure 10 presents the TCO breakdown for LLS architectures. In urban and sub-urban geo-types, L^{MW} shows consistent gain compared to fiber-based architectures mainly because of the lower cost of microwave and optical devices ($Ac_{\text{MW}} + Ac_{\text{opt}}$) compared to the fiber deployment and optical devices costs ($Ac_{\text{fib}} + Ac_{\text{opt}}$) in L_1^F, L_2^F, and L_3^F. However, in dense urban geo-type, the TCO of L^{MW} is comparable to fiber-based architectures. The average link length in dense urban is smaller than in urban and sub-urban areas, resulting in a low fiber deployment cost in the access segment (Ac_{fib}).

Also, in this case, we performed a sensitivity analysis varying the cost of fiber trenching and microwave devices. Figure 11 shows the TCO as a function of fiber trenching cost varied between ±60% of our benchmark (i.e., 2.4 [CU/m]) for the different discount levels of microwave devices, i.e., ±20% of our benchmark (BM) values in Table 3. In the sub-urban geo-type, L^{MW} has a lower TCO over the considered range of pricing for fiber trenching. On the other hand, the gain of using L^{MW} in dense urban and urban geo-types decreases with a decreasing value of the fiber trenching and an increased price of the microwave devices. Regardless of the TCO values, an operator might still prefer a microwave-based architecture for its shorter deployment time and easier installation/maintenance features.

F. LLS: latency and availability evaluation

As explained in Section 4, the average latency performance of an LLS architecture is evaluated considering the fronthaul latency requirements. Thus, l in Eq. (12) is equivalent to l_{LLS} in Eq. (9).

Figure 12 shows the average latency performance of the LLS architectures. The range of latency variation in the TN is small and all cell sites can meet the latency requirements of the eMBB and URLLC-T services (i.e., 0.1 [ms] and 0.05 [ms], respectively). With L^{MW}, a small percentage of cell sites cannot meet the latency requirement of URLLC-S service (i.e., 0.025 [ms]). A mix of technologies, including single-hop microwave and fiber, can be used for these specific cases. Besides, an operator may decide based on the trade-off between the number of sites meeting the latency requirement and other criteria such as TCO, time-to-market, and easier implementation of microwave technology. Usually, URLLC-S services will be present in some spots of the network and exist mainly in dense urban geo-types rather than outer areas.

Figure 13 shows the average availability performance of the LLS architectures. They can always provide an availability higher than 0.9999 in all geo-types and around 0.99999 for a percentage of sites.

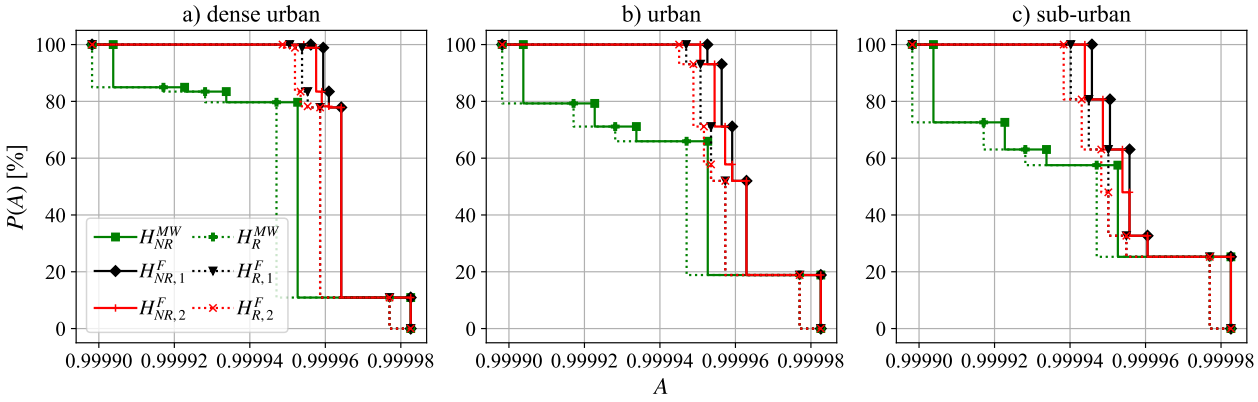

Fig. 9. HLS option: average availability performance.

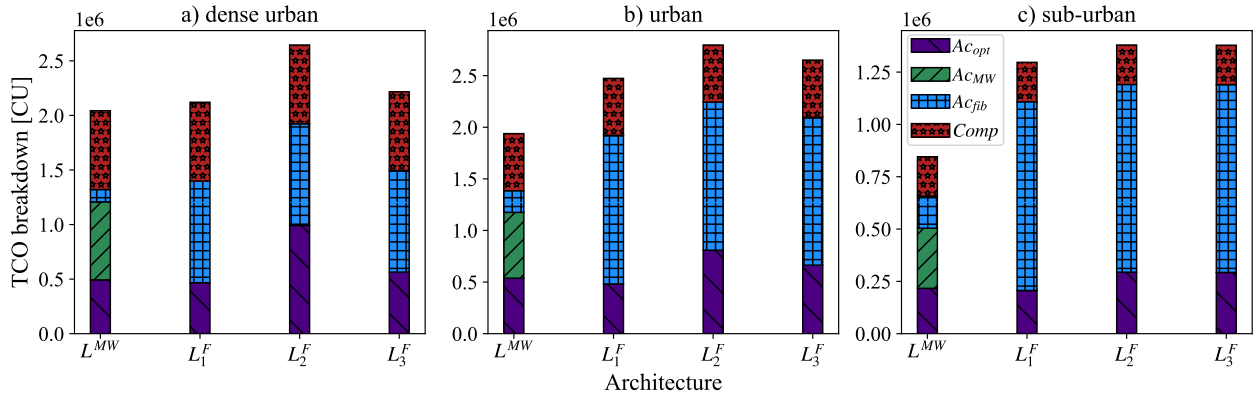

Fig. 10. LLS option: TCO breakdown for different geo-types.

6. CONCLUSIONS

This paper proposes a holistic framework to analyze a number of TN architectures using HLS and LLS options based on microwave and fiber technologies. We compared these architectures regarding TCO, latency, and connection availability in three geo-types (dense urban, urban, and sub-urban). We considered three services (eMBB, URLLC-T, and URLLC-S) with different latency and reliability requirements.

The study shows that with an HLS option, the microwave-based architecture under exam has lower TCO than their fiber-based counterparts. More specifically, the gain increases going from a dense urban to a sub-urban geo-type, where links are, on average, longer, leading to a higher fiber deployment cost. All considered architectures using HLS have almost similar average latency performance and can meet the user plane latency requirements of URLLC and eMBB services. The average availability performance of all the considered architectures is almost similar and within the range of the connection availability requirement of 3GPP.

In the case of an LLS option, the microwave-based architecture has a TCO value comparable to the fiber-based architectures in dense urban geo-types, while its TCO value is lower in urban and sub-urban geo-types. The microwave-based architecture can meet the latency requirements over the fronthaul for the eMBB and URLLC-T services. However, in the case of URLLC-S services, only single-hop microwave architectures can be used unless a minor latency performance degradation is acceptable. All LLS architectures (i.e., fiber- and microwave-based) have similar availability performance. In dense urban geo-types, it is important to note that the TCO gain of a microwave-based architecture (for both HLS and LLS) is affected by the cost of microwave equipment and fiber trenching. In summary, providing a univocal answer to the best technology for TN deployment is not easy. However, the results achieved in this study show that microwave is a good solution for 5G and beyond transport networks where microwave technology can meet the requirements of the different mobile network services. As a result, microwave can be considered an effective option where fiber rollout cannot meet the operator costs and deployment time objectives in different geo-types.

ACKNOWLEDGMENTS

This work was supported by the H2020 MSCA-ITN project 5G STEP FWD (grant 722429) and by the Smart City Concepts in Curitiba (2019-04893) project sponsored by VINNOVA (Sweden's innovation agency).

REFERENCES

1. Q. Chen, J. Wang, and H. Jiang, "URLLC and eMBB coexistence in MIMO non-orthogonal multiple access systems," arXiv:2109.05725 (2021).
2. 3GPP, "TR 38.801, study on new radio access technology: Radio access architecture and interfaces," Technical report (2017).
3. 3GPP, "TS 38.470, F1 general aspects and principles," Technical specification (2022).
4. O-RAN Open Fronthaul Interfaces Working Group 4, "Control, user and synchronization plane specification," Technical specification (2022).
5. T. Naveh, "Mobile backhaul: Fiber vs. microwave," Ceragon White Pap. **1**, 1–11 (2009).

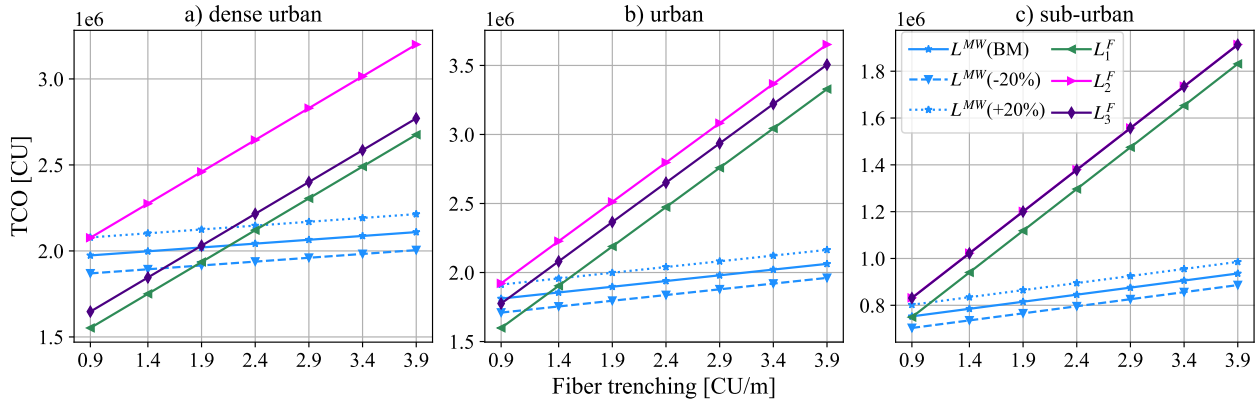

Fig. 11. LLS option: TCO variations while changing the fiber trenching and microwave equipment cost.

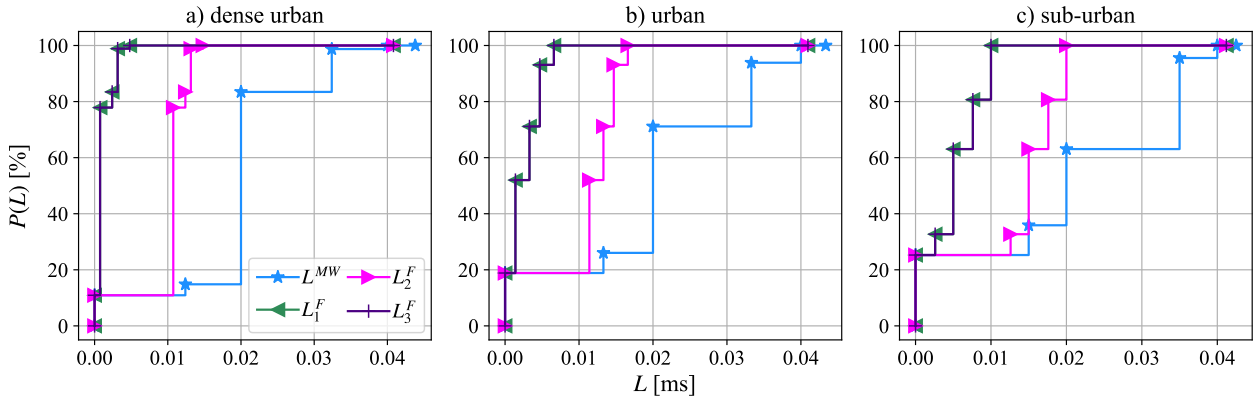

Fig. 12. LLS option: average latency performance.

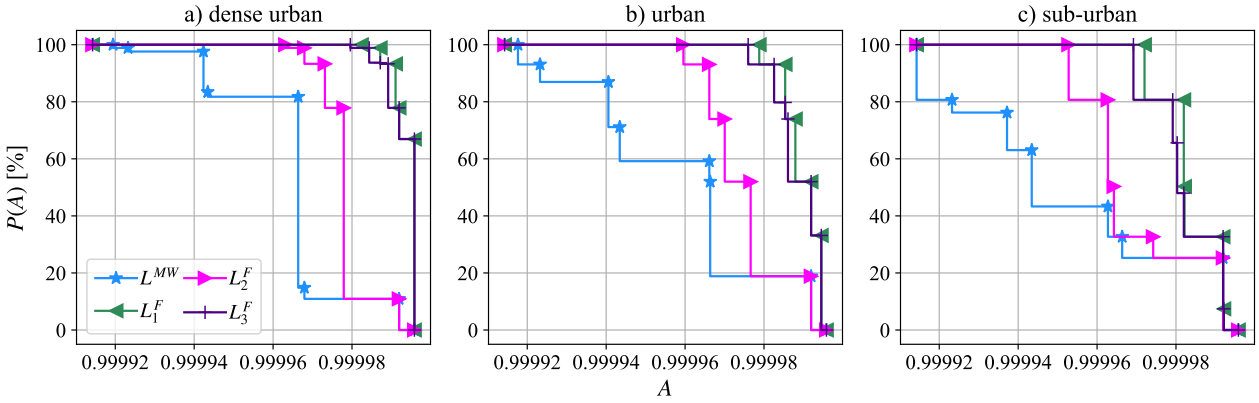

Fig. 13. LLS option : average availability performance.

6. F. Marzouk, M. Lashgari, J. P. Barraca, A. Radwan, L. Wosinska, P. Monti, and J. Rodriguez, *Virtual Networking for Lowering Cost of Ownership* (Springer International Publishing, Cham, 2022), pp. 331–369.
7. Next Generation Mobile Network (NGMN) Alliance, "5G white paper 2," White paper (2020).
8. E. J. Oughton, K. Katsaros, F. Entezami, D. Kaleshi, and J. Crowcroft, "An open-source techno-economic assessment framework for 5G deployment," IEEE Access **7**, 155930–155940 (2019).
9. F. Yaghoubi, M. Mahloo, L. Wosinska, P. Monti, F. d. S. Farias, J. C. W. A. Costa, and J. Chen, "A techno-economic framework for 5G transport networks," IEEE Wirel. Commun. **25**, 56–63 (2018).
10. H. Frank, R. S. Tessinari, Y. Zhang, Z. Gao, C. C. Meixner, S. Yan, and D. Simeonidou, "Resource analysis and cost modeling for end-to-end 5G mobile networks," in *International IFIP Conference on Optical Network Design and Modeling,* (Springer, 2019), pp. 492–503.
11. W. Xie, N.-T. Mao, and K. Rundberget, "Cost comparisons of backhaul transport technologies for 5G fixed wireless access," in *2018 IEEE 5G World Forum (5GWF),* (2018), pp. 159–163.
12. M. Lashgari, F. Tonini, M. Capacchione, L. Wosinska, G. Rigamonti, and P. Monti, "Fiber- vs. microwave-based 5G transport: a total cost of ownership analysis," in *European Conference on Optical Communication (ECOC) 2022,* (Optica Publishing Group, 2022), p. We1B.5.
13. S. Roblot, M. Hunukumbure, N. Varsier, E. Santiago, Y. Bao, S. Langouet, M.-H. Hamon, and S. Jeux, "Techno-economic analyses for vertical use cases in the 5G domain," arXiv:1906.09746 (2019).
14. I. Mesogiti, G. Lyberopoulos, F. Setaki, A. Di Giglio, A. Pelcelsi, L. Serra, J. Zou, A. Tzanakaki, M. Anastasopoulos, and E. Theodoropoulou, "Macroscopic and microscopic techno-economic analyses highlighting aspects of 5G transport network deployments," Photonic Netw.

Commun. **40**, 256–268 (2020).
15. O-RAN Open Xhaul Transport Working Group 9, "Xhaul packet switched architectures and solutions," Technical specification (2022).
16. ITU-T, "5G wireless fronthaul requirements in a passive optical network context," G-series recommendations, supplement 66 (2020).
17. J. S. Wey and J. Zhang, "Passive optical networks for 5G transport: Technology and standards," J. Light. Technol. **37**, 2830–2837 (2019).
18. L. M. P. Larsen, A. Checko, and H. L. Christiansen, "A survey of the functional splits proposed for 5G mobile crosshaul networks," IEEE Commun. Surv. Tutorials **21**, 146–172 (2019).
19. O-RAN Open Xhaul Transport Working Group 9, "Xhaul transport requirements," Technical specification (2021).
20. ITU-T, "Characteristics of transport networks to support IMT-2020/5G," G-series recommendations, 8300 (2020).
21. M. Lashgari, L. Wosinska, and P. Monti, "End-to-end provisioning of latency and availability constrained 5G services," IEEE Commun. Lett. **25**, 1857–1861 (2021).
22. J. Segovia, E. Calle, P. Vila, J. Marzo, and J. Tapolcai, "Topology-focused availability analysis of basic protection schemes in optical transport networks," J. Opt. Netw. **7**, 351–364 (2008).
23. Millimetre wave transmission ETSI industry specification group, "ETSI GR mWT 012, 5G wireless backhaul/x-haul," Group report (2018).
24. A. Udalcovs, M. Levantesi, P. Urban, D. A. A. Mello, R. Gaudino, O. Ozolins, and P. Monti, "Total cost of ownership of digital vs. analog radio-over-fiber architectures for 5G fronthauling," IEEE Access **8**, 223562–223573 (2020).
25. L. M. P. Larsen, H. L. Christiansen, S. Ruepp, and M. S. Berger, "deployment guidelines for cloud-RAN in future mobile networks," in *2022 IEEE 11th International Conference on Cloud Networking (CloudNet),* (2022), pp. 141–149.
26. F. Z. Morais, G. M. F. De Almeida, L. L. Pinto, K. Cardoso, L. M. Contreras, R. d. R. Righi, and C. B. Both, "PlaceRAN: optimal placement of virtualized network functions in beyond 5G radio access networks," IEEE Transactions on Mob. Comput. pp. 1–1 (2022).
27. "electricity prices," https://www.globalpetrolprices.com/electricity_prices/. Accessed on: 2023-01-29.
28. J. Mocerino, "5G backhaul/fronthaul opportunities and challenges," Technical paper (2019).
29. M. H. Keshavarz, M. Hadi, M. Lashgari, M. R. Pakravan, and P. Monti, "Optimal QoS-aware allocation of virtual network resources to mixed mobile-optical network slices," in *IEEE Global Communications Conference (GLOBECOM),* (2021), pp. 01–06.
30. 3GPP, "TS 38.211, physical channels and modulation," Technical specification (2022).
31. N. A. Johansson, Y.-P. E. Wang, E. Eriksson, and M. Hessler, "Radio access for ultra-reliable and low-latency 5G communications," in *IEEE International Conference on Communication Workshop (ICCW),* (2015), pp. 1184–1189.
32. ITU-R, "Availability objectives for real digital radio-relay links forming part of a high-grade circuit within an integrated services digital network," F-series recommendations, f.695 (1990).
33. H. Lehpamer, *Transmission systems design handbook for wireless networks*, Artech House mobile communications series (Artech House, 2002).
34. H. Long, M. Ye, G. Mirsky, A. D'Alessandro, and H. Shah, "Ethernet traffic parameters with availability information," RFC 8625 (2019).
35. 3GPP, "TS 22.104, service requirements for cyber-physical control applications in vertical domains," Technical specification (2021).

A. APPENDIX

The list of acronyms used in the paper are summarized in Table 5.

Table 5. List of acronyms.

BBU: baseband unit	MC: macrocell	PtP: point-to-point
CapEx: capital expenditure	MTTR: mean time to repair	ROADM: reconfigurable optical add-drop multiplexer
CU: cost unit	MTTF: mean time to failure	SC: small cell
DC: data center	MUX: multiplexer	TCO: total cost of ownership
DeMUX: de-multiplexer	MW: microwave	TN: transport network
eMBB: enhanced mobile broadband	ND: networking device	Tx/Rx: transceiver
FA: fiber aggregation	OADM: optical add-drop multiplexer	UE: user equipment
FDC: fiber deployment conversion	OpEx: operational expenditure	UP: user plane
HLS: high layer split	OTA: over-the-air	URLLC: ultra-reliable low latency communications
IRU: indefeasible right of use	PCU: power consumption unit	URLLC-S: URLLC-latency-sensitive
LLS: low layer split	PDN: passive distribution node	URLLC-T: URLLC-latency-tolerant
MA: metro aggregation	PON: passive optical network	